

GIRAF: General purpose In-storage Resistive Associative Framework

Leonid Yavits, Roman Kaplan and Ran Ginosar

Abstract—GIRAF is an in-storage architecture and algorithm framework based on Resistive Content Addressable Memory (RCAM). GIRAF functions simultaneously as a storage and a massively parallel associative processor. GIRAF alleviates the bandwidth wall by connecting every memory bit to processing transistors and keeping computing inside the storage arrays, thus implementing in-data, rather than near-data, processing. We show that GIRAF outperforms a reference computer architecture with a bandwidth-limited external storage access on a variety of data intensive workloads. The performance of GIRAF Euclidean distance, dot product and histogram implementation, exceeds the attainable performance of a reference architecture by up to four orders of magnitude, depending on the dataset size. The performance of GIRAF SpMV exceeds the attainable performance of such reference architecture by more than two orders of magnitude.

Index Terms—Near-data Processing; Associative Processing; Processing-in-storage; Processing-in-Memory; RRAM; CAM; Memristors.

1. INTRODUCTION

The premise of data centric, or near-data processing is reducing the memory access time by cutting the physical distance and increasing the bandwidth between processing units and memory. Since its inception, data centric processing mainly meant processing-in-memory (PIM). To process datasets larger than memory footprint, processing moves further down the memory hierarchy, achieving processing-in-storage.

In this paper, we propose a new General purpose In-data Resistive Associative Framework (GIRAF). We present the GIRAF architecture, programming model and application interface. GIRAF simultaneously functions as a data storage and a massively parallel fine-grain associative SIMD processor. GIRAF is based on Resistive Content Addressable Memory (RCAM). The processing is performed inside the storage arrays. There is no data transfer outside the storage arrays through a bandwidth limited interface to either a host CPU or a dedicated near-data processing unit. In GIRAF, every memory bit is directly connected to processing transistors, enabling ultra-high peak bandwidth and computation throughput while reducing the energy consumption, mainly attributed to reduction in data transfer.

This paper makes the following contributions:

- We introduce GIRAF, a General-purpose In-storage Resistive Associative Framework, which encompasses the architecture of a novel in-storage resistive associative processor, its programming model and its application interface.
- We develop GIRAF based implementation of several microbenchmarks and algorithms in the fields of machine learning, data analytics and graph processing.

- We show that GIRAF significantly outperforms a computer architecture with a bandwidth limited external data access while providing high power efficiency.

The rest of this paper is organized as follows. Section 2 introduces the architecture of GIRAF. Section 3 presents the principles of associative processing. Section 4 explores GIRAF programming and applications. Section 5 describes the evaluation methodology while Section 6 reports the experimental results. Section 7 presents the related work followed by discussion. Section 8 offers conclusions.

2. GIRAF Architecture

GIRAF employs resistive memory, organized in RCAM modules, as described here. Resistive memory stores information by modulating the resistance of nanoscale storage elements (memristors). Memristors are two-terminal devices, where the resistance of the device is changed by the electrical current or voltage. The resistance of the memristor is bounded by a minimum resistance R_{ON} (low resistive state, logic '1') and a maximum resistance R_{OFF} (high resistive state, logic '0').

The metal-oxide resistive random access memory (RRAM) is one of the leading candidates for next-generation nonvolatile storage [4]. Its main features are high endurance and fast access speed. A test-chip of 32Gb device with two RRAM-based memory layers and a CMOS logic layer underneath has been demonstrated [49].

RCAM is a scalable and highly dense alternative to CMOS CAM. A number of resistive CAM and ternary CAM cell designs have been proposed [5][23][51][52][73]. Our GIRAF architecture uses a resistive crossbar and additional peripheral circuitry (Figure 1) to support associative storage and processing.

- Leonid Yavits, E-mail: yavits@technion.ac.il.
- Roman Kaplan, E-mail: sromanka@campus.technion.ac.il
- Ran Ginosar, E-mail: ran@ee.technion.ac.il.

2.1 RCAM module

RCAM module, presented in Figure 1, is the heart of GIRAF architecture. It comprises a RRAM crossbar, in which each memory line is also a baseline processing unit (PU), and peripheral circuitry. The latter includes key and mask registers, TAG logic, and optional daisy-chain interconnect. The basic RCAM cell is created by virtually pairing two RRAM cells (memristors), holding complementary values R and \bar{R} .

The *key* register (Figure 1a) contains a key data word to be written or compared against. The *mask* register defines the active fields for write, compare and read operations, enabling bit selectivity. The *TAG* marks the rows that are matched by the compare operation and are to be affected by the successive parallel write. A daisy-chain like bitwise interconnect allows PUs to intercommunicate, all PUs in parallel.

RCAM compare operation is performed as follows. The Match/Word line is precharged and the key is set on Bit (key-not on Bit-not) lines. In the columns that are ignored during comparison, the Bit and Bit-not lines are asserted '1'. If all unmasked bits in a row match the key (*i.e.*, when Bit line '1' is applied to an R_{ON} memristor and Bit-not line '0' is applied to an R_{OFF} memristor, or vice versa), the Match/Word line remains high, and '1' is sampled into the corresponding tag bit. If at least one bit mismatches, the Match/Word line discharges through an R_{ON} memristor and '0' is sampled into the tag.

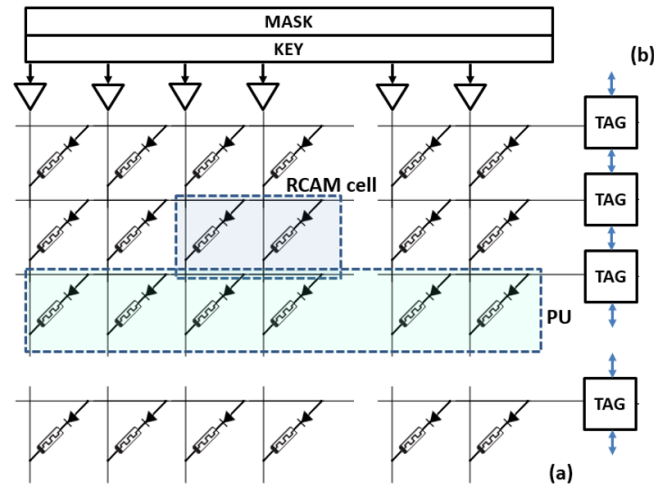


Figure 1: RCAM Module: (a) Resistive Crossbar and (b) Peripheral Circuitry.

Write operation is performed in two phases. First, the $V \geq V_{ON}$ voltage (where V_{ON} is a threshold voltage required to switch to the "on" state) is asserted to applicable Bit lines (to write '1's) and Bit-not lines (to write '0's). Second, the $V \leq V_{OFF}$ voltage (where V_{OFF} is a threshold voltage to switch to the "off" state) is asserted to Bit-not lines (to complement the '1's) and Bit lines (to complement '0's). The write affects only the tagged rows.

Memristor sub-nanosecond switching time [66][70] allows GHz operation. The energy consumption during compare may be 1fJ per bit [80]. The write energy is in the

100fJ per bit range [66][72][74], which may limit GIRAF single-chip scaling. The energy consumption is addressed in Section 6.

Another factor which potentially limits GIRAF is endurance (the number of program/write cycles that can be applied to a memristor before it becomes unreliable). Resistive memory endurance is shown at about 10^{12} [66][74], which may suffice for a few months of continuous operation.

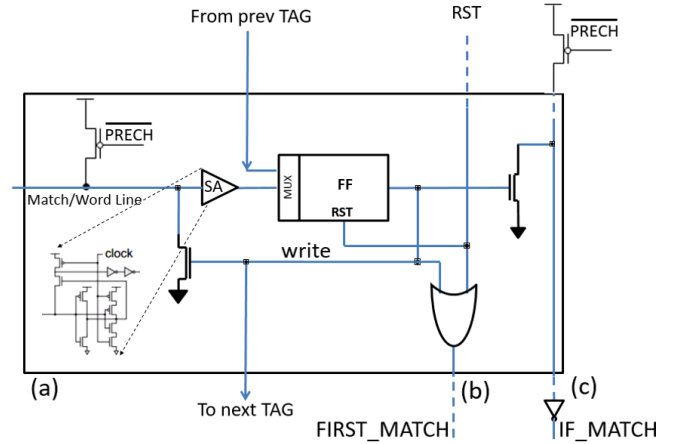


Figure 2. TAG Logic: (a) TAG, (b) First_match, (c) If_match.

2.1 Tag and Match Circuits

The TAG logic is presented in Figure 2. It comprises a pre-charge transistor, a Match line sense amplifier, a TAG flip-flop, a multiplexer (part of the daisy-chain tag connectivity), a first_match circuit and an if_match circuit. The Match line is pre-charged during compare. The TAG flip-flop holds the result of compare. The First_match circuit implements 'first_match', a frequent associative operation, by keeping only the first matching tag and resetting the remaining tags (Section 4.2). If_match, another frequent associative operation, returns '1' if compare operation results in at least one match.

2.2 System Architecture and GIRAF scaling

Conceptually, GIRAF may comprise billions and trillions of rows (PUs). Due to timing and thermal considerations, GIRAF is divided into multiple daisy-chained RCAM modules, possibly implemented by separate ICs.

GIRAF controller is responsible for managing the processing operations of GIRAF. It issues instructions, sets the key and mask registers, handles control sequences and executes read requests. In addition, it contains a data buffer, which stores the reduction tree outputs. The controller may also perform some baseline processing.

The scaling of conventional near-data processing architectures may be limited, similarly to parallel manycore von Neumann architectures. When the growing storage size and internal bandwidth of the storage arrays are met by the increasing number of in-storage processing cores, the communication among them may become a bottleneck. As a result, the performance of a conventional

processing-in-storage system may saturate or even diminish.

GIRAF is relatively simple to scale just by cascading RCAM modules. Daisy-chain connectivity allows an easy partitioning of GIRAF into separate ICs. The inherent parallelism of GIRAF allows increasing the performance of many workloads almost linearly as the datasets grow along with storage size. Since the bulk of data is never transferred outside the storage arrays through a bandwidth-limited interface, the performance limit is pushed further away.

3. Associative Processing

Associative processor (AP) is a non-von-Neumann in-memory computer [76]. AP is based on CAM, which allows comparing the entire dataset to a search pattern (key), tagging the matching row, and writing another pattern to all tagged rows. AP performs no computations in conventional sense. Most arithmetic and logic operations can be structured as series of Boolean functions, which are implemented by the AP as follows.

The dataset is stored in CAM, typically one data element per CAM row (constituting a Processing Unit, PU). AP controller sequentially matches all possible *input* combinations of a function arguments against the entire CAM content. The matching CAM rows are tagged, and the corresponding function values (precalculated and embedded in AP microcode), are written into the designated *output* fields of the tagged rows.

For an m -bit argument x ($x \in \text{dataset}$), any Boolean function $b(x)$ has at most 2^m possible values (“at most” because of “don’t cares”). Therefore, a brute-force approach would incur up to $O(2^m)$ cycles, regardless of the dataset size.

More efficiently, arithmetic operations can be performed in GIRAF in a word-parallel, bit-serial manner, reducing time complexity from $O(2^m)$ to $O(m)$. For instance, vector addition may be performed as follows [25]. Suppose that two m -bit RCAM columns hold vectors A and B; the sum $S=A+B$ is written onto another m -bit column S (Figure 3). A one-bit column C holds the carry bit. The operation is carried out as m single-bit additions (1):

$$c[:,i] | s[:,i] = a[:,i] + b[:,i] + c[:,i], \quad i = 0, \dots, m-1 \quad (1)$$

where i is the bit index, ‘:’ means all elements of the vector, and c and s are, respectively, the carry and sum bits. The single-bit addition is carried out in a series of steps. In each step, one entry of the full adder truth table (a three bit input pattern, Figure 3(a)) is matched against the contents of the $a[:,i], b[:,i], c[:,i]$ bit columns and the matching rows (PUs) are tagged; the logic result (two-bit output of the truth table, Figure 3(a)) is written into the $c[:,i]$ and $s_i[:,i]$ bits of all tagged rows. During that operation, all but three input bit columns and two output bit columns of RCAM are masked out in each step. Overall, eight steps of one compare and one write operation are performed to complete a single-bit addition over all RCAM rows (i.e. over all vector elements), regardless of the vectors A and B lengths.

A snapshot of such vector addition, for $m = 4$, zero bit of the vector elements and the 2nd entry of the truth table is shown in Figure 3. Figure 3(a) shows the truth table with the 2nd entry marked out. Figure 3(b) and (c) show compare and write operations respectively, against the backdrop of the RCAM map (with two 4-bit input vectors occupying bit-columns 0-3 and 4-7 respectively). The 4-bit output vector S is reserved columns 8-11, while bit column 12 is used for storing and updating the carry bit C.

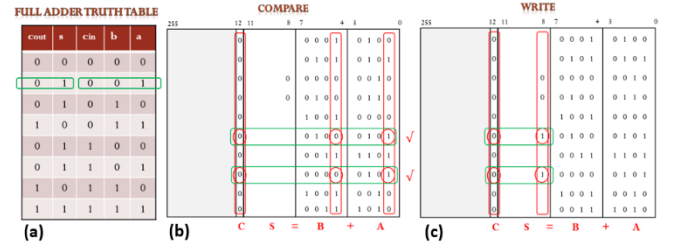


Figure 3: Vector addition in RCAM example, for two 4-bit vectors A and B, snapshot at zero bit, 2nd entry of the truth table: (a) Full Adder Truth Table, (b) Compare, only c, a₀ and b₀ are affected, (c) Write, only c and s₀ in the tagged rows (PUs) are affected

During compare (Figure 3(b)), the input pattern ‘001’ is compared against bit columns c, a₀ and b₀, for all vector elements in parallel. The matching rows (two in this example) are tagged. During write (Figure 3(c)), the output pattern ‘01’ is written in bit columns c and s₀ accordingly. Only the tagged rows are written. Each compare and write affect the entire dataset (vectors A, B and S).

A fixed-point m bit addition and subtraction take $O(m)$ cycles. Fixed point multiplication and division in GIRAF require $O(m^2)$ cycles. Single precision floating point multiplication takes 4,400 cycles [78], regardless of the dataset size.

4. Programming and applications

In this section, we briefly present GIRAF data organization, instruction set and programming model. Afterwards, we discuss the implementation of several data-intensive workloads from different application fields, such as machine learning, data analytics, linear algebra and graph processing.

Somewhat less ambitious applications include basic data mining operations such as *grep* and *string matching*, addressed by several near-data processing-in-storage architectures [41][58]. Clearly, whereas the complexity of reading data out of storage arrays for performing search by in-SSD cores (or a host processor) is of linear time complexity, performing search in GIRAF is closer to constant time complexity, and is not addressed in this work.

4.1 GIRAF Data Organization

GIRAF typically places one data element per RCAM row. Such data element normally occupies only a part of the row, while the rest of it is used for temporary storage. For example, in 128-bit wide row, data element may

occupy bits 0 through 63, while bits 64 through 127 might be reserved for temporary variables or used in associative arithmetic operations.

Data in associative memory is accessed by its content rather than its address. Data elements of the same dataset are normally identified by a unique index, or a class member ID. RRAM and RCAM, unlike DRAM, do not require a fixed, page-sized data allocation to operate efficiently. Therefore, individual data elements do not have to be placed in any specific order (unless it is required by the algorithm, such as in SpMV (section 4.4.3), in which case the reordering time is taken into account). They may rather be scattered in random sparse locations (rows) within the RCAM array, although typically in the same bit columns (fields).

4.2 GIRAF Associative Instruction Set

In this section, we present the main GIRAF associative instructions.

1. **compare** ($y1==x1, y2==x2, \dots, yn==xn$). Compares the key x (stored in the key register) to the field y (masked by mask register) in the entire RCAM array.
2. **write** ($y1=x1, y2=x2, \dots, yn=xn$). Writes the value x stored in the key register to the field y (masked by mask register) in the entire RCAM array. Write affects only the tagged RCAM rows (could be multiple rows).
3. **read** (y). Reads field y (masked by mask register) from a tagged RCAM row to the key register.
4. **if_match**. Signals "1" if there is at least one match in the entire RCAM array.
5. **first_match**. Reset all tags set by compare but the first (top-most) one.

4.3 Programming GIRAF

An external host may run an operating system and sequential code, and delegate processing-in-storage tasks to GIRAF. GIRAF implements these tasks as parallel SIMD kernels. A user is responsible for analyzing each application to identify the highly parallelizable data intensive SIMD parts. The user further divides such application into sequential compute intensive parts (executed in the host) and massively parallel data intensive fractions (executed by GIRAF). The code intended to run in GIRAF is translated into associative primitives that are downloaded into and executed by the GIRAF controller. Presently, GIRAF code is manually encoded at assembly language level.

The host invokes GIRAF to perform its code fraction. The host uses memory-mapped registers to communicate with GIRAF through the host CPU - GIRAF interface. The host transfers parameters such as data starting addresses, kernel configuration starting addresses, and kernel ID and triggers kernel execution/reconfiguration on GIRAF by writing to the kernel registers. Once GIRAF starts the execution, it can access the parameters from those registers. GIRAF can notify the host of its execution status by writing to the status registers. The host periodically polls these memory-mapped status registers to check for kernel completion or exceptions. The status register read

by the host does not intervene in GIRAF operation. Based on the kernel running on GIRAF and the dataset size of the kernel, the host can accurately estimate the execution time of a kernel, thereby polling status when the kernel execution is about to finish. Once GIRAF execution completes, the host can access the GIRAF output.

There is no hardware support for data coherence between the host CPU and GIRAF. GIRAF has no access to the host main memory or on-chip cache. Therefore, the datasets on which GIRAF operates must reside in GIRAF and should not be left in the host memory. To avoid inconsistencies between the GIRAF and host memory, GIRAF storage is inaccessible to the host during GIRAF operation.

4.4 Applications

The focus of GIRAF is large scale data intensive applications, i.e., applications with very high bandwidth requirements, and with datasets that do not fit in a typical main memory. We perform a case study on a number of data intensive workloads from four important big-data application domains, as follows.

4.4.1 Machine Learning Primitives

Euclidean distance calculation is a frequent bottleneck in clustering algorithms (e.g., K-means), where the distances between each one of a number of cluster centers and each one of a multitude of multidimensional (multi-attribute) samples (X) are calculated iteratively.

Figure 4 presents a fully associative algorithm for Euclidean distance calculation in GIRAF. The samples are assumed to be stored in GIRAF, an attribute per RCAM row.

Algorithm 1 Euclidean Distance

```

// X: the group of samples; samples are not required to be
// placed in any specific order prior to execution;
// n: number of centers
// Every  $x \in X$  is stored in a separate RCAM row
// Each of the  $n$  cluster centers: ( $i_{center}, Center$ )
1. For each  $i_{center} \in [1, n]$ : //  $i_{center}$  is used as ID to
   // associatively mark the relevant samples
2. Do-all  $x \in X$ : // at all RCAM rows in parallel
3. Write  $center$  coordinates to  $temp$  column
4. For each  $attr \in \{sample\ attributes\}$ :
5.    $dist_{attr} \leftarrow x_{attr} - center_{attr}$ 
6.    $sqEucDist_{attr} \leftarrow (dist_{attr})^2$  // Associative mult
7.    $sqEucDist_{to_{center}} \leftarrow sqEucDist_{to_{center}} +$ 
       $sqEucDist_{attr}$ 

```

Figure 4: GIRAF based Euclidean distance calculation

All arithmetic operations (sub, add, square) are implemented associatively, in bit-serial manner, as series of compare and write commands. Lines 1-3 are performed in parallel for all attributes of all samples. Lines 4-7 are executed attribute by attribute, in parallel for all samples. The Euclidean distance calculation time does not depend on the number of samples, only on their dimensions.

Dot product calculation is a recurring bottleneck in classification algorithms, such as Support Vector Machine,

which iteratively calculates dot product between a hyperplane vector H and a multitude of vectors X .

Figure 5 presents a fully associative algorithm for dot product calculation. The vectors are assumed to be stored in GIRAF.

Algorithm 2 Dot product

```
// X: input vectors of size n; Vectors are not required
// to be placed in any specific order prior to
// execution;
// H: Hyperplane vector
// Every x ∈ X is stored in a separate RCAM row
1. For each i ∈ [1, n]: // i is used as ID to
   // associatively mark the relevant elements
2. Do-all x ∈ X: // at all RCAM rows in parallel
3. Multi ← xi × Hi // Associative mult
4. DPi = DPi + Multi // Associative add
```

Figure 5: GIRAF based dot product calculation

Arithmetic operations (multiply and add) are implemented associatively, in bit-serial manner. The ‘For’ loop in line 1 is performed in parallel for all vectors. The dot product calculation time hence does not depend on the number of vectors, only on their size.

4.4.2 Data Analytics

We calculate a m -bin histogram from 32-bit data (stored as a vector of size n). We further present a fully associative histogram calculation algorithm (Figure 6). We set $m = 256$ to allow a single-operation 1-byte shift to generate a bin index in an in-host implementation of histogram, used for comparison to GIRAF implementation. The 32-bit samples are assumed to be stored in GIRAF, a sample per RCAM row.

Algorithm 3 Histogram

```
// X: the group of samples; samples are not required
// to be placed in any specific order prior to
// execution; m: number of bins
// Every x ∈ X is stored in a separate RCAM row
1. For each ibin ∈ [1, m]: // ibin is used as ID to
   // associatively mark the relevant samples
2. Do-all x ∈ X: // at all RCAM rows in parallel
3. compare ibin to the bits [31...24] of x
4. Hibin ← Reduction(tagged rows)
```

Figure 6: GIRAF based histogram calculation

4.4.3 Linear Algebra

Sparse matrix by vector multiplication (SpMV) is a data intensive kernel widely used across the entire spectrum of machine learning algorithms. We propose a fully associative algorithm for SpMV execution in GIRAF. Revised versions of this algorithm can be used for dense matrix multiplication and sparse matrix by matrix [78] multiplication.

Figure 7 presents the algorithm of GIRAF SpMV. Matrix A is assumed to be stored in GIRAF in Compressed Sparse Row (CSR) format, where each nonzero element e_A is stored alongside its column index i_A .

The algorithm includes three parts. The first part, broadcast, consists of a loop going over the elements of vector B . In the first cycle, the index of an element of B , i_B , is compared against the column index field of the entire matrix A (in parallel for all nonzero elements of A , using the compare command). All index-matching rows holding nonzero elements of matrix A are tagged.

In the second cycle, B element e_B is written simultaneously into all tagged rows, alongside the index-matched elements of matrix A . The loop is repeated for all elements of vector B . Upon completion, each nonzero pair of elements of A and B required to calculate the product vector C is aligned (stored in the same row) in the RCAM.

The second part (step 4) is the associative multiplication of the e_A, e_B pairs, performed associatively in parallel for all pairs. The number of multiplications performed simultaneously equals the number of nonzero elements in A .

The third part sums the products along each row of A (lines 5, 6) using soft reduction, which is performed in parallel for all output vector C elements, where for each such element, we accumulate the partial products in a binary tree fashion: first, all odd and even partial products are summed up; then the odd and even partial results are summed up, and so on, until the last pair of partial results are summed up. Soft reduction requires (1) placing of odd and even partial products and results in the same PU, and (2) adding them up.

GIRAF SpMV has the computational complexity of $O(n_A)$ where n_A is the matrix dimension (assuming square matrix for simplicity).

Algorithm 4 SpMV

```
// Let A, B, C denote matrix A and vectors B and C.
// Each RCAM row holds a non-zero element of A (eA, iA)
// Matrix elements are not required to be placed in any
// specific order prior to execution;
// Broadcast
1. For each eB ∈ {elements of B}:
   // Compare iB with all column indices of A, iA
2. Compare iB to all iA
   // Write eB into all matching rows
3. Write eB
   // Associatively multiply the entire A by B
4. PR ← eB * eA // PR is a matrix
   // Reduction: all rows of A in parallel, each row is tallied
5. For each (non-zero) row k of A:
6. Ck ← Reduction(PRk)
   // C has non-zero elements where A has non-zero rows
```

Figure 7: GIRAF based SpMV pseudocode.

4.4.4 Large-Scale Graph Processing

Breadth first search (BFS) is an algorithm for traversing or searching graphs. BFS GIRAF row mapping is presented in Table 1.

Table 1. BFS Data Format and GIRAF Row Mapping

Bits 0-47	Bits 48-95	Bit 96	Bit 97	Bits 98-145	Bits 146-153
Vertex ID	Successor ID	Visited Bit	Visited From Bit	Predecessor ID	Distance

The pseudocode of GIRAF serial implementation of BFS is presented in Figure 8.

5. Evaluation Methodology

5.1 Simulator and Hardware Design

We implemented a custom cycle-accurate simulator for GIRAF. The simulator is used for design space exploration and RTL verification.

To measure the area, power and timing of GIRAF logic circuits, we synthesized the TAG logic (Figure 2) using Synopsis Design Compiler with the 45nm FreePDK open cell library and scaled the area and power figures to 28nm technology. A 256×128 RCAM array was laid-out manually using Cadence Virtuoso. The energy and timing figures of RCAM array were obtained using SPICE simulation with TEAM model [45].

Algorithm 5 BFS

```

// Source vertex has distance set to 0
// All visited_bit set to 0
// All visited_from_bit set to 0
1. j = -1;
2. j++;
3. do {
4.   compare [distance == j, visited_from_bit == 0];
5.   if (if_match == 0) go to (2);
6.   first_match;
7.   write [visited_from_bit = 1]; // marks current vertex as
                                "visited from"
8.   read [vertexID, successorID, visited_bit]; // successors'
                                                visited_bit
9.   do for all with visited_bit==0 {
10.    compare [vertexID == successorID];
11.    write [distance = j+1, predecessorID = vertexID,
            visited_bit = 1]; // updates all successors
12.  } // do in (9)
13.  compare [visited_bit == 0]; //check if non-visited remain
14.  if (if_match == 0) break; //finish: break main loop
15. } // do in (3)

```

Figure 8: Serial BFS pseudocode

5.2 Baseline for Comparison

GIRAF is a processing-in-storage architecture, capable of internally maintaining the entire dataset. The alternative is a computer architecture (either data centric or CPU centric) where the dataset does not fit in internal memory, therefore requiring an external storage. Such external storage could either be a SSD, a NVDIMM based storage [34], or a dedicated storage appliance [35]. The bandwidth of such external storage is typically limited. For example, a storage appliance may be limited by bandwidth of 10GB/s

[35]. NVDIMM storage typically provides higher, although also limited bandwidth, for example 24GB/s [34].

The performance of such architecture is defined by the roofline model [71] as follows:

$$\text{Attainable Perf} = \min(\text{Peak Perf}, AI \times \text{Peak Storage BW}) \quad (2)$$

where *Peak Perf* is the peak theoretical performance of the computer architecture, *AI* is arithmetic (or operational) intensity of a workload, and *Peak Storage BW* is the peak external storage bandwidth (as demonstrated in Figure 12). In data intensive applications, characterized by low *AI*, the attainable performance of an architecture is typically limited by its peak storage bandwidth. Therefore $AI \times \text{Peak Storage BW}$ is the performance baseline for our evaluation. We present GIRAF performance figures relative to the attainable performance of said baseline architecture, assuming both the storage appliance and NVDIMM storage scenarios.

6. Experimental Results

6.1 Area

A single TAG cell area in 28nm is 7.1 μm^2 , and its average energy consumption is 5.6fJ. The RCAM array area is 452.2 μm^2 in 28nm. GIRAF is simulated at the operating frequency of 500MHz.

6.2 Performance and Energy

We simulate Euclidean distance calculation in GIRAF using a number of synthetic vectors of sizes of 1M, 10M and 100M. Euclidean distance requires three floating point operations per each data access (to fetch a vector attribute), assuming that center values and resulting Euclidean distance values are stored locally in the host. Assuming single precision floating point, arithmetic intensity of Euclidean distance calculation is $AI = 3/4 \left[\frac{FLOP}{B} \right]$. The attainable performance of Euclidean distance calculation is 7.5GFLOPS for a storage appliance and 18GFLOPS for a NVDIMM storage, although the peak theoretical performance of a reference computer architecture could be much higher. The normalized Euclidean distance performance is shown in Figure 9. The power efficiency of GIRAF Euclidean distance implementation is 2.9 GFLOPS/W.

Dot product calculation in GIRAF is simulated using synthetic 16-dimensional vectors, with the number of vectors of sizes of 1M, 10M and 100M. The attainable performance of Dot product calculation is 5GFLOPS for a storage appliance and 12GFLOPS for a NVDIMM storage. The normalized dot product performance is shown in Figure 9. The power efficiency of GIRAF dot product implementation is 2.7 GFLOPS/W.

We simulate a 256-bin histogram calculation in GIRAF using synthetic 32-bit integer vectors, with vector sizes of 1M, 10M and 100M. The attainable performance of Euclidean distance calculation is 7.5GFLOPS for a storage appliance and 18GFLOPS for a NVDIMM storage. The normalized histogram performance is shown in Figure 9.

The power efficiency of GIRAF histogram implementation is 2.4 GFLOPS/W.

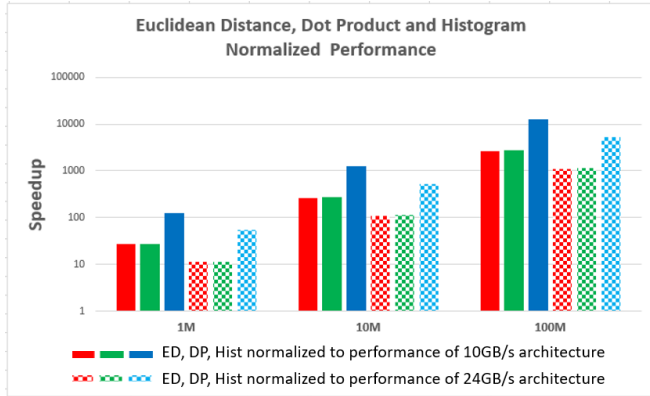


Figure 9: GIRAF Normalized Performance for Euclidean Distance (ED), Dot Product (DP) and Histogram (Hist)

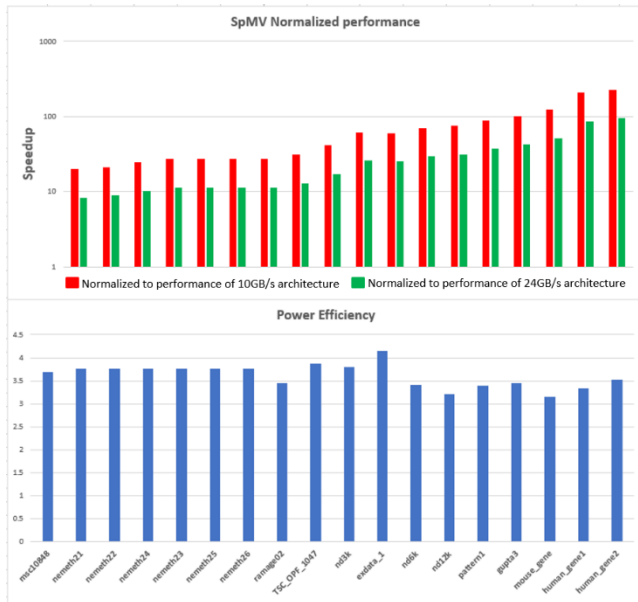


Figure 10: GIRAF SpMV (a) Normalized Performance, (b) Power Efficiency

To simulate sparse matrix multiplication, we used 18 square matrices from the UFL Sparse Matrix Collection [17] (listed in Figure 10), having 1.2 through 29 million nonzero elements. The normalized SpMV performance is presented in Figure 10(a). The results are presented in the order of increasing matrix density, expressed as $\frac{nmz_A}{n_A}$ where n_A is the matrix dimension and nmz_A is the number of nonzero elements. GIRAF relative performance grows with matrix density because all multiplications of vector elements by nonzero matrix elements are done in GIRAF SpMV in parallel. The simulated power efficiency of the SpMV is presented in Figure 10(b). It ranges from 3 to 4GFLOPS/W.

We simulate BFS using the graphs presented in Table 2. We measure BFS performance in Traversed Edges Per

Second (TEPS). The attainable performance of BFS is 2.5GTEPS for a storage appliance and 6GTEPS for a NVDIMM storage, although the peak theoretical performance of a reference computer architecture could be much higher. GIRAF BFS performance is presented in Figure 11. The results are presented in the order of increasing average out-degree (Avg D).

Table 2. Graphs Used in Evaluation

Graph	V [M]	E [M]	Avg D	Max D
indochina-2004	5.3	79	15	19409
arabic-2005	23	640	28	575,618
it-2004	41	1151	28	1,326,745
sk-2005	50.6	1,949	38	8,563,808
kron_g500-logn21	2.1	182	87	213,905
hollywood-09	1.1	114	100	11,468

V-vertices, E-edges, D- out-degree; Vertices and edges are in [Millions]

For all workloads examined here, GIRAF performance is limited by the density of the problem (rather than by bandwidth as in the baseline architecture). Euclidean distance and dot product are examples of dense problems (the entire dataset is processed simultaneously), where GIRAF yields the best performance. In SpMV, performance is a function of matrix density. The denser the matrix (meaning more multiply-accumulate operations simultaneously), the better the performance. In BFS, GIRAF achieves only up to 7 times better performance than external storage bandwidth-limited architectures, due to its serial implementation (vertices are examined serially and the speedup is limited by the average out-degree of the graph).

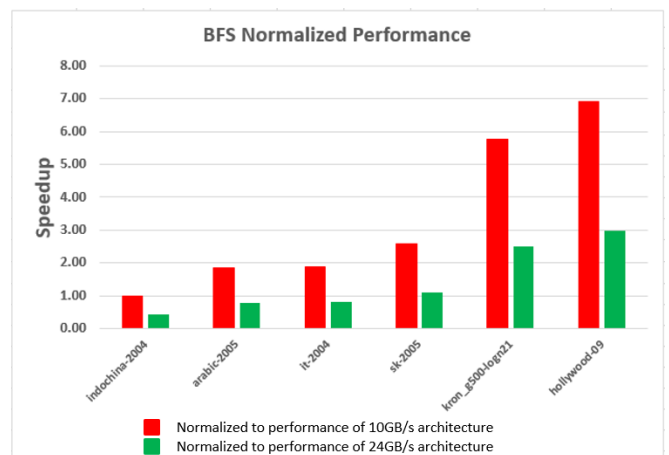


Figure 11. GIRAF BFS Normalized Performance

Near-data processing architectures may enable external bandwidth considerably higher than 10GB/s or 24GB/s. For example, Tesseract [1] combines massively parallel multicore processor with a 3D memory cube, targeting a peak bandwidth of 8TB/s. However, the bandwidth of such 3D processing-in-memory architecture is still ultimately limited by serial interfaces, vertical interconnects and the

rest of the communication infrastructure connecting memory layers to the processing layer. In contrast, processing in GIRAF is carried out in every memory row in parallel, hence its peak theoretical bandwidth is not constrained by memory to processing unit connectivity. Moreover, GIRAF bandwidth scales linearly with the memory size. Assuming that GIRAF scales with the dataset size, and provided a dataset large enough, GIRAF can conceptually outperform any 3D-integrated processing-in-memory architecture.

6.3 Peak Theoretical Bandwidth and Performance

The peak potential of GIRAF (with 4TB of storage in this example) is illustrated using the roofline model in Figure 12. It shows the roofline model of GIRAF against the backdrop of Intel’s KNL [20], to which we add an external storage appliance access. Since GIRAF requires no external storage access, its attainable performance is defined by its peak internal bandwidth and its peak performance.

The peak internal bandwidth is achieved for instance during a transfer of an entire bit column to the TAG register. Another example is the broadcast of a single data item to the entire storage (e.g., the broadcast in SpMV, Figure 7). The peak performance is calculated using a single precision floating point multiply-accumulate operation, performed in parallel on the entire dataset (assuming the dataset matches the GIRAF size, i.e. 1T 32bit data elements).

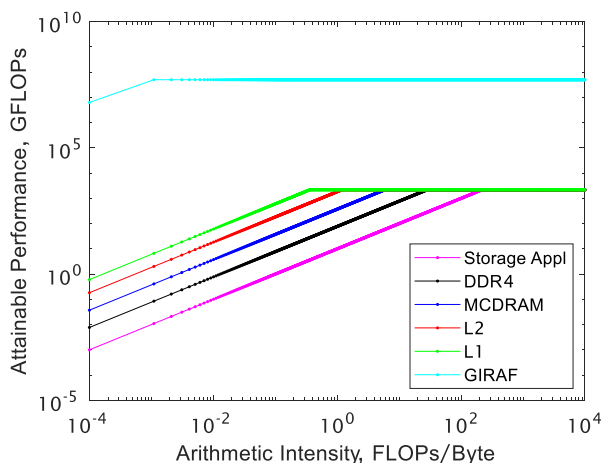


Figure 12: Roofline model based on [20], amended by BW chart of an external storage appliance and a model for 4TB GIRAF.

7. Related Work and Discussion

The related work is divided into processing-in-memory vs. processing-in-storage (SSD), and near-data vs. in-data processing categories. Processing-in-memory includes cache and DRAM whereas storage relates mostly to non-volatile memory and SSD. In near-data processing systems, processing cores are placed close to the data, whereas in-data processing refers to compute circuitry being intertwined with memory. A comprehensive review

of data centric processing architectures and trends can be found in [9].

7.1 Near-Data Processing-In-Memory

While processing-in-storage (SSD) research is relatively young, near-data processing-in-memory (PIM) has been thoroughly researched. The concept of mixing memory and logic has been around since 1960s. The DAPP, STARAN, CM-2, and GAPP computer architectures [60] used large number of PUs positioned in proximity to memory arrays to implement a massively parallel SIMD computer. Gokhale *et al.* [27] designed TeraSys, a computer architecture comprising a conventional host processor where at least part of its memory was replaced by a PIM array, integrating memory and ALUs in close proximity. Hall *et al.* [32] developed DIVA, the Data-Intensive Architecture, combining PIM memories with external host processors and performing selected computations in processing elements near memory and reducing the volume of data transferred across the long and slow processor-memory interface. Almasi *et al.* [6] developed Cyclops, an architecture combining memory and a large number of simple PUs. Sterling *et al.* [67] developed Gilgamesh, a PIM based massively parallel architecture, focusing on advanced mechanisms for virtualizing tasks and data. Kogge *et al.* [43] developed HTMT, a parallel multilevel memory architecture, where each RAM level is a PIM memory (memory blocks interconnected with ALUs). Suh *et al.* [68] introduced a SLIIC QL computer featuring a processor integrated on the same die as DRAM. Brockman *et al.* [12] developed PIM lite, a PIM architecture featuring a multithreaded core with SIMD accelerator integrated with DRAM on the same chip.

7.2 3D Based Processing-In-Memory

While embedding processing with conventional 2D DRAM chips is less practical, recent advancement in 3D memory and logic stacking technology may remove this obstacle. A wide variety of 3D DRAM cube / logic stack based processing-in-memory designs have been proposed. Ahn *et al.* [1] introduced Tesseract, a 3D Processing in Memory accelerator for large-scale graph processing. In another work, Ahn *et al.* [2] developed a hybrid memory cube based framework that automatically decides whether to execute PIM operations in host or memory depending on data locality patterns. Nair, Sura *et al.* [57][69] introduced the Active Memory Cube, a heterogeneous computing system including general-purpose host processors and specially designed in-memory processors that would be integrated in a logic layer within 3D DRAM memory. Gao *et al.* [53] developed hardware and software of a 3D stack memory and near-data processing architecture for in-memory analytics frameworks, including MapReduce, graph processing, and deep neural networks. Azarkhish *et al.* [7] developed Smart Memory Cube and designed a high bandwidth interconnect to serve the bandwidth demand of PIM architecture. Zhang *et al.* [79] explored PIM implemented via 3D die stacking. Akin *et al.* [3] addressed the issue of data reorganization in 3D stacked near-data processing architecture, introducing

HAMLeT, a mechanism for host interference, bandwidth allocation, and in-memory coherence. Farmahini-Farahani *et al.* [24] proposed NDA, a near-DRAM acceleration architecture that processes data using accelerators 3D-stacked on DRAM devices.

The main difference between GIRAF and a 3D near-data processing architectures is the bitwise connectivity of memory and processing: In GIRAF, each memory bit is directly connected to processing transistors, whereas in 3D near-data processing, the data must pass through memory interface circuits and through vertical interconnects, typically much fewer in numbers than the number of bits. In GIRAF, the bulk of data never leaves the memory. The computation is performed within the confines of the memory array. Moreover, the peak bandwidth of GIRAF scales with the dataset and memory size. This potentially holds a significant performance and energy efficiency advantage: Using DRAM as example, there is typically a reduction in available bandwidth of six orders of magnitude between the sense amplifiers and the CPU edge [9]. In addition, the cost of access in terms of energy increases from hundreds of femtojoules to tens of picojoules over a span of the same distance [9].

7.3 In-Data Processing-In-Memory

In-data processing-in-memory developed in parallel with near-data processing-in-memory research. Lipovsky *et al.* [48] introduced DAAM, a dynamic associative access memory architecture that combined DRAM and a single-bit processing element, capable of associative and conventional arithmetic processing, placed in the sense amplifier area of a DRAM. Yavits *et al.* [77] suggested replacing the last level cache and the vector co-processor of a conventional high-performance CPU by an associative processor, which is a PIM accelerator, combining data storage and massively parallel SIMD processing capabilities. Morad *et al.* introduced GP-SIMD [54], a two-dimensional processing-in-memory architecture featuring a scalar host processor and a single bit vector processor.

Recently, emerging memory technologies such as resistive memory have become a focus of PIM research. Somnath *et al.* [59] developed M_{BARC}, a resistive crossbar in-memory LUT-based processing architecture. Chi *et al.* [13] introduced PRIME, a PIM accelerator of neural network applications. Yavits *et al.* [76] presented ReAP, a resistive CAM based massively parallel associative accelerator. Morad *et al.* [55] introduced Re-GP-SIMD, a two-dimensional resistive processing-in-memory accelerator. Shafiee *et al.* [65] developed ISAAC, an in-situ accelerator of neural network, where memristor crossbar arrays are used to perform dot-product operations in an analog manner. Kvatinsky *et al.* [63] and Talati *et al.* [56] developed MAGIC, a RRAM based in-data processing-in-memory architecture. Hamdioui *et al.* [33] introduced CIM, a memristor based computation in memory architecture. Bojnordi and Ipek [11] introduced Memristive Boltzmann machine, a hardware accelerator for combinatorial optimization and deep learning. Imani *et al.* [37] introduced APIM, an approximate processing in-memory architecture which exploits the analog characteristics of

resistive memory to support addition and multiplication inside the crossbar.

7.4 Near-Data Processing-In-Storage

Typical processing-in-storage architecture places a single or several processing cores inside the storage (with main focus on NAND flash solid-state disk) and allows data processing without transferring it to the host processor. Boboila *et al.* [10] proposed Active Flash, a processing in solid-state storage that expedites data analysis by migrating the data to the flash device. The authors explored energy and performance trade-offs of their processing-in-storage architecture. Bae *et al.* [8] introduced the notion of Intelligent SSDs, exploring the design considerations and examining their potential benefits in data mining applications. Continuing the work on Intelligent SSD, Jo *et al.* [38] studied optimal ways of combining CPU, GPU and SSD for efficient processing of data-intensive algorithms. Cho *et al.* [14] cited the lack of parallel processing abilities in earlier in-SSD processing architectures and proposed integrating a GPU, providing API sets based on the MapReduce framework. Kang *et al.* [41] introduced the Smart SSD model, which combines in-SSD processing with a powerful host system and constructed a Smart SSD prototype. De *et al.* [19] introduced the FPGA-based Minerva, which executed application-specific operations in the NVM controller. Jun *et al.* [39] introduced and constructed BlueDBM, combining a flash based storage with in-store processing capability and a low latency high-throughput inter-controller network, and explored its performance benefits. Cho *et al.* [15] explored some of the questions which are also addressed by this paper. The authors made a case for Intelligent SSD by discussing the bandwidth trends and quantifying the potential benefits of processing-in-storage across a range of applications.

7.5 Processing in Resistive CAM and TCAM

The use of STT-MRAM and Resistive Ternary CAM for data intensive computing was pioneered by Guo *et al.* [29][30][31]. Guo *et al.* used the associative capabilities of CAM and Ternary CAM for search operations, while the computing is largely done in a near-TCAM CPU. Adopting associative processing architectures such as Goodyear Aerospace's STARAN or MPP to processing-in-storage is also suggested in [9].

8. Conclusions

We propose GIRAF, a General purpose In-data Resistive Associative Framework, based on Resistive Content Addressable Memory (RCAM). Unlike conventional near-data architectures, GIRAF enables storage with *in-data* associative processing capabilities. GIRAF can contain billions and trillions of data rows, with each row serving as an in-data associative processing unit. GIRAF requires no data transfer outside the storage arrays. Each memory bit of GIRAF is directly connected to processing transistors, thus providing an ultra-high peak memory bandwidth, which scales linearly with GIRAF size.

GIRAF, capable of general purpose associative processing, has been applied to a variety of challenging data intensive problems in data analytics, machine learning and graph processing. The paper investigated Euclidian distance, dot product, histogram, Sparse Matrix-Vector multiplication and BFS and performed performance and power efficiency analysis of GIRAF.

REFERENCES

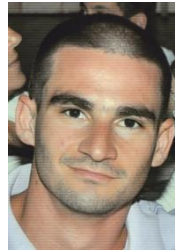
- [1] Ahn, J., Hong, S., Yoo, S., Mutlu, O., and Choi, K., "A scalable processing-in-memory accelerator for parallel graph processing," *Computer Architecture (ISCA), ACM/IEEE 42nd Annual International Symposium on*, pp. 105–117 2015.
- [2] Ahn, J., Yoo, S., Mutlu, O., & Choi, K. "PIM-enabled Instructions: A Low-overhead, Locality-aware Processing-in-memory Architecture." *Computer Architecture (ISCA) ACM/IEEE 42nd Annual International Symposium on* (pp. 336-348), 2015.
- [3] Akin, B., Franchetti, F., & Hoe, J. C.. "HAMLeT architecture for parallel data reorganization in memory". *IEEE Micro*, 36(1), 14-23, 2016.
- [4] Akinaga, H., and Hisashi Shima. "Resistive random access memory (RRAM) based on metal oxides." *Proceedings of the IEEE* 98.12: 2237-2251, 2010.
- [5] Alibart, F., T. Sherwood, D. Strukov. "Hybrid CMOS/nanodevice circuits for high throughput pattern matching applications", *IEEE Conference on Adaptive Hardware and Systems*, 2011.
- [6] Almási, G., C. Caşcaval, J. G. Castanos, M. Denneau, D. Lieber, J. E. Moreira, and H. S. Warren Jr, "Dissecting cyclops: A detailed analysis of a multithreaded architecture," *ACM SIGARCH Computer Architecture News*, vol. 31, no. 1, pp. 26–38, 2003.
- [7] Azarkhish, E., Pfister, C., Rossi, D., Loi, I. and Benini, L. "Logic-Base Interconnect Design for Near Memory Computing in the Smart Memory Cube". *IEEE Transactions on Very Large Scale Integration (VLSI) Systems*, 25(1), 210-223, 2017.
- [8] Bae, D.-H., J.-H. Kim, S.-W. Kim, H. Oh, and C. Park, "Intelligent SSD: a turbo for big data mining," in *Proceedings of the 22nd ACM international conference on Conference on information & knowledge management*, pp. 1573–1576, ACM, 2013.
- [9] Balasubramonian, R., Chang, J., Manning, T., Moreno, J. H., Murphy, R., Nair, R., & Swanson, S. "Near-data processing: Insights from a MICRO-46 workshop", *IEEE Micro*, 34(4), 36-42, 2013.
- [10] Boboila, S., Kim, Y., Vazhkudai, S. S., Desnoyers, P., & Shipman, G. M. (2012, April). Active flash: Out-of-core data analytics on flash storage. In *Mass Storage Systems and Technologies (MSST), IEEE 28th Symposium on* (pp. 1-12), 2012.
- [11] Bojnordi, M. N., & Ipek, E. (2016, March). Memristive boltzmann machine: A hardware accelerator for combinatorial optimization and deep learning. In *High Performance Computer Architecture (HPCA), 2016 IEEE International Symposium on* (pp. 1-13).
- [12] Brockman, J. B., Thoziyoor, S., Kuntz, S. K., and Kogge, P. M., "A low cost, multithreaded processing-in-memory system," *Proceedings of the 3rd workshop on Memory performance issues: in conjunction with the 31st international symposium on computer architecture*, pp. 16–22, 2004.
- [13] Chi, P., Li, S., Xu, C., Zhang, T., Zhao, J., Liu, Y., Wang, Y., and Xie, Y., "Prime: A novel processing-in-memory architecture for neural network computation in reram-based main memory," *Proceedings of the 43rd International Symposium on Computer Architecture*, pp. 27–39, IEEE Press, 2016.
- [14] Cho, B. Y., W. S. Jeong, D. Oh and W. W. Ro, "Xsd: Accelerating mapreduce by harnessing the gpu inside an ssd," *Proceedings of the 1st Workshop on Near-Data Processing* 2013.
- [15] Cho, S., Park, C., Oh, H., Kim, S., Yi, Y., and Ganger, G. R. "Active disk meets flash: A case for intelligent ssds," in *Proceedings of the 27th international ACM conference on International conference on supercomputing*, pp. 91–102, 2013.
- [16] Coburn, J., Bunker, T., Schwarz, M., Gupta, R., & Swanson, S. From ARIES to MARS: Transaction support for next-generation, solid-state drives. In *Proceedings of the twenty-fourth ACM symposium on operating systems principles*, pp. 197-212, 2013.
- [17] Davis, T., Hu, Y., "The University of Florida sparse matrix collection," *ACM Transactions on Mathematical Software (TOMS)*, 38, no. 1, 2011.
- [18] de Oliveira Sandes, E. F., Miranda, G., Martorell, X., Ayguade, E., Teodoro, G., & Melo, A. C. M. CUDAlign 4.0: Incremental Speculative Traceback for Exact Chromosome-Wide Alignment in GPU Clusters. *IEEE Transactions on Parallel and Distributed Systems*, 27(10), 2838-2850, 2016.
- [19] De, A., M. Gokhale, R. Gupta, and S. Swanson, "Minerva: Accelerating data analysis in next-generation ssds," in *Field-Programmable Custom Computing Machines (FCCM), 2013 IEEE 21st Annual International Symposium on*, pp. 9–16, IEEE, 2013.
- [20] Doerfler, Douglas, et al. "Applying the roofline performance model to the intel xeon phi knights landing processor." *International Conference on High Performance Computing*. Springer International Publishing, 2016.
- [21] Duck-Ho, B., Jin-Hyung, K., Yong-Yeon, J., Sang-Wook, K., Hyunok, O., & Chanik, P. Intelligent SSD: A turbo for big data mining. *Proceedings of the 22nd ACM international conference on Conference on information & knowledge management*, 2013, pp. 1573-1576, 2016.
- [22] Elliott, D. G., Stumm, M., Snelgrove, W. M., Cojocaru, C., & McKenzie, R. (1999). *Computational RAM: Implementing processors in memory*. *IEEE Design & Test of Computers*, 16(1), 32-41.
- [23] Eshraghian, K., Cho, K. R., Kavehei, O., Kang, S. K., Abbott, D., & Kang, S. M. S. Memristor MOS content addressable memory (MCAM): Hybrid architecture for future high performance search engines. *IEEE Transactions on Very Large Scale Integration (VLSI) Systems*, 19(8), 1407-1417, 2011.
- [24] Farmahini-Farahani, A., Ahn, J. H., Morrow, K., & Kim, N. S. "NDA: Near-DRAM acceleration architecture leveraging commodity DRAM devices and standard memory modules." *IEEE International Symposium on High Performance Computer Architecture (HPCA)*, pp. 283-295, 2015.
- [25] Foster, C., "Content Addressable Parallel Processors", Van Nostrand Reinhold Company, NY, 1976.
- [26] Gao, M., and Kozyrakis, C. (2016, March). "HRL: efficient and flexible reconfigurable logic for near-data processing." *IEEE International Symposium on High Performance Computer Architecture (HPCA)*, (pp. 126-137).
- [27] Gokhale, M., Holmes, B. and Iobst, K. "Processing in memory: The terasys massively parallel pim array," *Computer*, vol. 28, no. 4, pp. 23–31, 1995.
- [28] Gotoh, O. "An improved algorithm for matching biological sequences." *Journal of molecular biology* 162.3, pp. 705-708, 1982.
- [29] Guo, Q., Guo, X., Bai, Y., and Ipek, E. A resistive TCAM accelerator for data-intensive computing. *Proceedings of the 44th Annual IEEE/ACM International Symposium on Microarchitecture*, pp. 339-350, 2011.
- [30] Guo, Q., Guo, X., Bai, Y., Patel, R., Ipek, E., and Friedman, E. G. "Resistive ternary content addressable memory systems for data-intensive computing." *IEEE Micro*, vol. 35, no. 5, pp. 62-71, 2015.
- [31] Guo, Q., Guo, X., Patel, R., Ipek, E., & Friedman, E. G. "AC-DIMM: associative computing with STT-MRAM". *ACM SIGARCH Computer*

- Architecture News, vol. 41, no. 3, pp. 189-200, 2013.
- [32] Hall, M., Kogge, P., Koller, J., Diniz, P., Chame, J., Draper, J., LaCoss, J., Granacki, J., Brockman, J., Srivastava, A. and Athas, W. "Mapping irregular applications to DIVA, a PIM-based data-intensive architecture". Proceedings of the 1999 ACM/IEEE conference on Supercomputing, p. 57, 1999.
- [33] Hamdioui, Said, Lei Xie, Hoang Anh Du Nguyen, Mottaqiallah Taouil, Koen Bertels, Henk Corporaal, Hailong Jiao et al. "Memristor based computation-in-memory architecture for data-intensive applications." In Proceedings of the 2015 Design, Automation & Test in Europe Conference & Exhibition, pp. 1718-1725. EDA Consortium, 2015.
- [34] <https://www.micron.com/-/media/documents/products/data-sheet/modules/nvdimms/ddr4/asf18c2gx72pflz.pdf>
- [35] <https://www-01.ibm.com/common/ssi/cgi-bin/ssialias?htmlfid=TSD03191USEN>
- [36] Imani, M., Kim, Y., & Rosing, T. (2017, January). Mpim: Multi-purpose in-memory processing using configurable resistive memory. In Design Automation Conference (ASP-DAC), 2017 22nd Asia and South Pacific (pp. 757-763). IEEE.
- [37] Imani, Mohsen, Saransh Gupta, and Tajana Rosing. "Ultra-Efficient Processing In-Memory for Data Intensive Applications." Proceedings of the 54th Annual Design Automation Conference 2017. ACM, 2017.
- [38] Jo, Y. Y., Cho, S., Kim, S. W., & Oh, H. "Collaborative processing of data-intensive algorithms with CPU, intelligent SSD, and GPU." Proceedings of the 31st Annual ACM Symposium on Applied Computing, pp. 1865-1870, 2016.
- [39] Jun, S. W., Liu, M., Lee, S., Hicks, J., Ankcorn, J., King, M., Xu, S, Arvind, "BlueDBM: an appliance for big data analytics", ACM/IEEE 42nd Annual International Symposium on Computer Architecture (ISCA), 2015.
- [40] Kang, Y., Huang, W., Yoo, S. M., Keen, D., Ge, Z., Lam, V., ... & Torrellas, J. (2012, September). FlexRAM: Toward an advanced intelligent memory system. In Computer Design (ICCD), 2012 IEEE 30th International Conference on (pp. 5-14). IEEE.
- [41] Kang, Y., Kee, Y. S., Miller, E. L., & Park, C. (2013, May). Enabling cost-effective data processing with smart SSD. IEEE 29th Symposium on Mass Storage Systems and Technologies (MSST), pp. 1-12, 2013.
- [42] Kepner, Jeremy, and John Gilbert, eds. Graph algorithms in the language of linear algebra. Society for Industrial and Applied Mathematics, 2011.
- [43] Kogge, P. M., Brockman, J., and Freeh, V. W. "Pim architectures to support petaflops level computation in the htmt machine," International Workshop on Innovative Architecture for Future Generation High-Performance Processors and Systems, pp. 35-44, IEEE, 2000.
- [44] Krizhevsky, A., I. Sutskever, and G. E. Hinton, "ImageNet Classification with Deep Convolutional Neural Networks," Advances in Neural Information Processing Systems 25 (F. Pereira, C. Burges, L. Bottou, and K. Weinberger, eds.), pp. 1097-1105, Curran Associates, Inc., 2012.
- [45] Kvatinisky, S., Friedman, E. G., Kolodny, A., & Weiser, U. C. (2013). TEAM: Threshold adaptive memristor model. IEEE Transactions on Circuits and Systems I: Regular Papers, 60(1), 211-221.
- [46] Lee, V. T., del Mundo, C. C., Alaghi, A., Ceze, L., Oskin, M., & Farhadi, A. (2016). NCAM: Near-Data Processing for Nearest Neighbor Search. arXiv preprint arXiv:1606.03742.
- [47] Li, S., Xu, C., Zou, Q., Zhao, J., Lu, Y., & Xie, Y. (2016, June). Pinatubo: A processing-in-memory architecture for bulk bitwise operations in emerging non-volatile memories. In IEEE Design Automation Conference (DAC), 2016 53rd ACM/EDAC/IEEE (pp. 1-6).
- [48] Lipovski, G. J., and Yu, C. "The dynamic associative access memory chip and its application to simd processing and full-text database retrieval," in Records of the IEEE International Workshop on Memory Technology, Design and Testing, pp. 24-31, 1999.
- [49] Liu, T. Y., Yan, T. H., Scheuerlein, R., Chen, Y., Lee, J. K., Balakrishnan, G. and Sasaki, T. A 130.7nm² 32-Gb ReRAM Memory Device in 24-nm Technology. IEEE Journal of Solid-State Circuits, 49(1), 140-153, 2014.
- [50] Lowe, D. G. "Distinctive Image Features from Scale-Invariant Keypoints," Int. J. Comput. Vision, vol. 60, pp. 91-110, Nov. 2004.
- [51] Matsunaga, S., Hiyama, K, Matsumoto, A, Ikeda, S, Hasegawa, H, Miura, K, Hayakawa, J., Endoh, T., Ohno, H., and Hanyu, T. "Standby-power-free compact ternary content-addressable memory cell chip using magnetic tunnel junction devices." Applied Physics Express 2, no. 2, 2009.
- [52] Matsunaga, S., Katsumata, A., Natsui, M., Fukami, S., Endoh, T., Ohno, H., and Hanyu, T., "Fully Parallel 6T-2MTJ Nonvolatile TCAM with Single-Transistor-Based Self Match-Line Discharge Control," Symposium on VLSI Circuits Digest of Technical Papers, pp. 298-299, 2011.
- [53] Mingyu, G., Ayers, G., and Kozyrakis, C. "Practical near-data processing for in-memory analytics frameworks." International Conference on Parallel Architecture and Compilation (PACT), 2015.
- [54] Morad, A., Yavits, L., & Ginosar, R. (2015). GP-SIMD processing-in-memory. ACM Transactions on Architecture and Code Optimization (TACO), 11(4), 53.
- [55] Morad, A., Yavits, L., Kvatinisky, S., & Ginosar, R. (2016). Resistive GP-SIMD processing-in-memory. ACM Transactions on Architecture and Code Optimization (TACO), 12(4), 57.
- [56] N. Talati, S. Gupta, P. Mane, and S. Kvatinisky, "Logic design within memristive memories using memristor-aided loGIC (MAGIC)," *IEEE Trans. Nanotechnol.*, vol. 15, no. 4, pp. 635-650, 2016.
- [57] Nair, R., Antao, S.F., Bertolli, C., Bose, P., Brunheroto, J.R., Chen, T., Cher, C.Y., Costa, C.H., Doi, J., Evangelinos, C. and Fleischer, B.M. "Active memory cube: A processing-in-memory architecture for exascale systems. IBM Journal of Research and Development," 59(2/3), pp.17-1, 2015.
- [58] Park, K., Kee, Y. S., Patel, J. M., Do, J., Park, C., & Dewitt, D. J. "Query Processing on Smart SSDs". IEEE Data Eng. Bull., 37(2), 19-26, 2014.
- [59] Paul, S., & Bhunia, S. A scalable memory-based reconfigurable computing framework for nanoscale crossbar. IEEE transactions on Nanotechnology, 11(3), 451-462, 2012.
- [60] Potter J., and Meilander, W. "Array processor supercomputers," Proceedings of the IEEE, vol. 77, no. 12, pp. 1896-1914, 1989.
- [61] Ramanathan, N., Wickerson, J., Winterstein, F., & Constantinides, G. A. A case for work-stealing on fpgas with opencd atomics. Proceedings of the ACM/SIGDA International Symposium on Field-Programmable Gate Arrays (pp. 48-53), 2016.
- [62] Rossbach, C. J., Yuan Yu, Jon, C., Jean-Philippe M., and Dennis F. "Dandelion: a compiler and runtime for heterogeneous systems." Proceedings of the Twenty-Fourth ACM Symposium on Operating Systems Principles, pp. 49-68. 2013.
- [63] S. Kvatinisky et al., "MAGIC—Memristor-Aided Logic," *IEEE Trans. Circuits Syst. II Express Briefs*, vol. 61, no. 11, pp. 895-899, 2014.
- [64] Saule, E., Kaya, K., & Çatalyürek, Ü. V. Performance evaluation of sparse matrix multiplication kernels on intel xeon phi. In International Conference on Parallel Processing and Applied Mathematics (pp. 559-570), 2013.
- [65] Shafiee, A., Nag, A., Muralimanohar, N., Balasubramonian, R., Strachan, J.P., Hu, M., Williams, R.S. and Srikumar, V., ISAAC: A convolutional neural network accelerator with in-situ analog arithmetic in crossbars. In Proceedings of the 43rd International Symposium on Computer Architecture (pp. 14-26), 2016.
- [66] Shulaker, Max M., Gage Hills, Rebecca S. Park, Roger T. Howe, Krishna

Saraswat, H.S. Philip Wong, and Subhasish Mitra. "Three-dimensional integration of nanotechnologies for computing and data storage on a single chip." *Nature* 547, no. 7661 (2017): 74-78.

- [67] Sterling, T. L. and Zima, H. P., "Gilgamesh: A multithreaded processor-in-memory architecture for petaflops computing," *Supercomputing, ACM/IEEE 2002 Conference*, pp. 48-48, IEEE, 2002.
- [68] Suh, J., Li, C., Crago, S. P., and Parker, R. "A pim-based multiprocessor system," *Proceedings of 15th International Parallel and Distributed Processing Symposium*, pp. 6-pp, IEEE, 2001.
- [69] Sura, Z., Jacob, A., Chen, T., Rosenburg, B., Sallénave, O., Bertolli, C., Antao, S., Brunheroto, J., Park, Y., O'Brien, K. and Nair, R., May. Data access optimization in a processing-in-memory system. In *Proceedings of the 12th ACM International Conference on Computing Frontiers*, p. 6, 2015.
- [70] Torrezan, A. C., Strachan, J. P., Medeiros-Ribeiro, G., & Williams, R. S. "Sub-nanosecond switching of a tantalum oxide memristor." *Nanotechnology*, vol. 22 no. 48, 2011.
- [71] Williams, S., Waterman, A., & Patterson, D. (2009). Roofline: an insightful visual performance model for multicore architectures. *Communications of the ACM*, 52(4), 65-76.
- [72] Wouters, D. J., Waser, R., & Wuttig, M. (2015). Phase-change and redox-based resistive switching memories. *Proceedings of the IEEE*, 103(8), 1274-1288.
- [73] Xu, W., Zhang, T., Chen, Y., "Design of spin-torque transfer magnetoresistive RAM and CAM/TCAM with high sensing and search speed", *IEEE Transactions VLSI Systems*, 18.1 pp. 66-74, 2010.
- [74] Yang, J., Strukov, D., and Stewart, D. "Memristive devices for computing." *Nature nanotechnology*, vol. 8, no. 1, 13-24, 2013.
- [75] Yavits L, Morad, A., & Ginosar, R. "The effect of communication and synchronization on Amdahl's law in multicore systems". *Parallel Computing*, vol. 40, no. 1, pp. 1-16, 2014.
- [76] Yavits, L., Kvatinisky, S., Morad, A., & Ginosar, R. (2015). Resistive associative processor. *IEEE Computer Architecture Letters*, 14(2), 148-151.
- [77] Yavits, Leonid, Amir Morad, and Ran Ginosar. "Computer architecture with associative processor replacing last-level cache and SIMD accelerator." *IEEE Transactions on Computers* 64.2 (2015): 368-381.
- [78] Yavits, Leonid, Amir Morad, and Ran Ginosar. "Sparse matrix multiplication on an associative processor." *IEEE Transactions on Parallel and Distributed Systems* 26.11 (2015): 3175-3183.
- [79] Zhang, D., Jayasena, N., Lyashevsky, A., Greathouse, J. L., Xu, L., & Ignatowski, M. TOP-PIM: Throughput-oriented programmable processing in memory. *Proceedings of the 23rd international symposium on High-performance parallel and distributed computing*, pp. 85-98, 2014.
- [80] Madhavan, A., Sherwood, T., & Strukov, D. B. (2018). High-Throughput Pattern Matching With CMOL FPGA Circuits: Case for Logic-in-Memory Computing. *IEEE Transactions on Very Large Scale Integration (VLSI) Systems*, (99), 1-14.

He co-authored a number of patents and research papers on SoC and ASIC. His research interests include non von Neumann computer architectures and processing in memory.



Roman Kaplan (M'17) received his BSc and MSc from the faculty of Electrical Engineering, Technion, Israel in 2009 and 2015, respectively. He is now a PhD candidate in the same faculty under the supervision of Prof. Ran Ginosar. Kaplan's research interests are parallel computer architectures, in-data processing, accelerators for machine learning and big data, and novel computer architectures for bioinformatics applications.



Ran Ginosar (M'78) received his BSc from the Technion—Israel Institute of Technology in 1978 (summa cum laude) and his PhD from Princeton University, USA, in 1982, both in Electrical and Computer Engineering. His Ph.D. research focused on shared-memory multiprocessors. He worked at AT&T Bell Laboratories in 1982-1983, and joined the Technion faculty in 1983. He was a visiting Associate Professor with the University of Utah in 1989-1990, and a visiting faculty with Intel Research Labs in 1997-1999. He is a Professor at the Department of Electrical Engineering and serves as Head of the VLSI Systems Research Center at the Technion. His research interests include VLSI architecture, manycore computers, asynchronous logic and synchronization, networks on chip and biologic implant chips. He has co-founded several companies in various areas of VLSI systems.



Leonid Yavits received his MSc and PhD in Electrical Engineering from the Technion. After graduating, he co-founded VisionTech where he co-designed a single chip MPEG2 codec. Following VisionTech's acquisition by Broadcom, he co-founded Horizon Semiconductors where he co-designed a

Set Top Box on chip for cable and satellite TV. Leonid is a postdoc fellow in Electrical Engineering in the Technion.